


# Proline isomerization modulates the bacterial IsdB/hemoglobin interaction: an atomic force spectroscopy study

Francesca Pancrazi<sup>1</sup>  · Omar De Bei<sup>2</sup>  · Francesco Lavecchia di Tocco<sup>1</sup>  · Marialaura Marchetti<sup>2</sup>  · Barbara Campanini<sup>3</sup>  · Salvatore Cannistraro<sup>1</sup>  · Stefano Bettati<sup>2,4</sup>  · Anna Rita Bizzarri<sup>1</sup> 

Received: 11 September 2024 / Accepted: 6 January 2025

Published online: 07 February 2025

© The Author(s) 2025 

## Abstract

Iron surface determinant B (IsdB), a *Staphylococcus aureus* (SA) surface protein involved in both heme iron acquisition from host hemoglobin (Hb) and bacterial adhesion, is a proven virulence factor that can be targeted for the design of antibacterial molecules or vaccines. Recent single-molecule experiments on IsdB interaction with cell adhesion factors revealed an increase of the complex lifetime upon applying a stronger force (catch bond); this was suggested to favor host invasion under shear stress. An increased bond strength under mechanical stress was also detected by Atomic Force Spectroscopy (AFS) for the interaction between IsdB and Hb. Structural information on the underlying molecular mechanisms at the basis of this behaviour in IsdB-based complexes is missing. Here, we show that the single point mutation of Pro173 in the IsdB domain responsible for Hb binding, which weakens the IsdB:Hb interaction without hampering heme extraction, totally abolishes the previously observed behavior. Remarkably, Pro173 does not directly interact with Hb, but undergoes *cis-trans* isomerization upon IsdB:Hb complex formation, coupled to folding-upon binding of the corresponding protein loop. Our results suggest that these events might represent the molecular basis for the stress-dependence of bond strength observed for wild type IsdB, shedding light on the mechanisms that govern the capability of SA to infect host cells.

## 1 Introduction

The mechanisms regulating the interaction between pathogenic bacteria and human host cells are the result of adaptive processes developed in course of evolution to reach a fast and efficient acquisition of essential nutrients able to guarantee the bacterium survival [1]. The understanding of these mechanisms is crucial to develop new strategies to fight pathogens, especially in the perspective to overcome the worldwide emergence arising from antibiotic resistance acquired by several microorganisms [2]. *Staphylococcus aureus* (SA) is a pathogenic bacterium that can give rise to severe human infections affecting e.g. skin, respiratory apparatus, circulatory system, and the heart, often with fatal consequences [3]. SA exhibits a high propensity to acquire antibiotic resistance, and the design of new drugs able to block or to weaken its interaction with human cells is becoming a high priority. To infect host cells, SA exploits different virulence factors with a large involvement of cell wall-anchored (CWA) proteins which promote bacterial adhesion and internalization, biofilm

Francesca Pancrazi and Omar De Bei have contributed equally.

✉ Stefano Bettati, stefano.bettati@unipr.it; ✉ Anna Rita Bizzarri, bizzarri@unitus.it | <sup>1</sup>Biophysics and Nanoscience Centre, DEB, Università della Tuscia, Largo dell'Università, 01100 Viterbo, Italy. <sup>2</sup>Department of Medicine and Surgery, University of Parma, Via Volturno 39, 43125 Parma, Italy. <sup>3</sup>Department of Food and Drug, University of Parma, Parco Area delle Scienze 23/A, 43124 Parma, Italy. <sup>4</sup>Institute of Biophysics, National Research Council, via G. Moruzzi, 56124 Pisa, Italy.



**Fig. 1** A schematic representation of Isd system from *S. aureus*. **b** Three-dimensional structure of IsdB NEAT1 domain free in solution (Protein Data Bank (PDB) id 2MOQ). **c** Three-dimensional structure of IsdB NEAT1 bound to Hb (PDB id 7PCH)

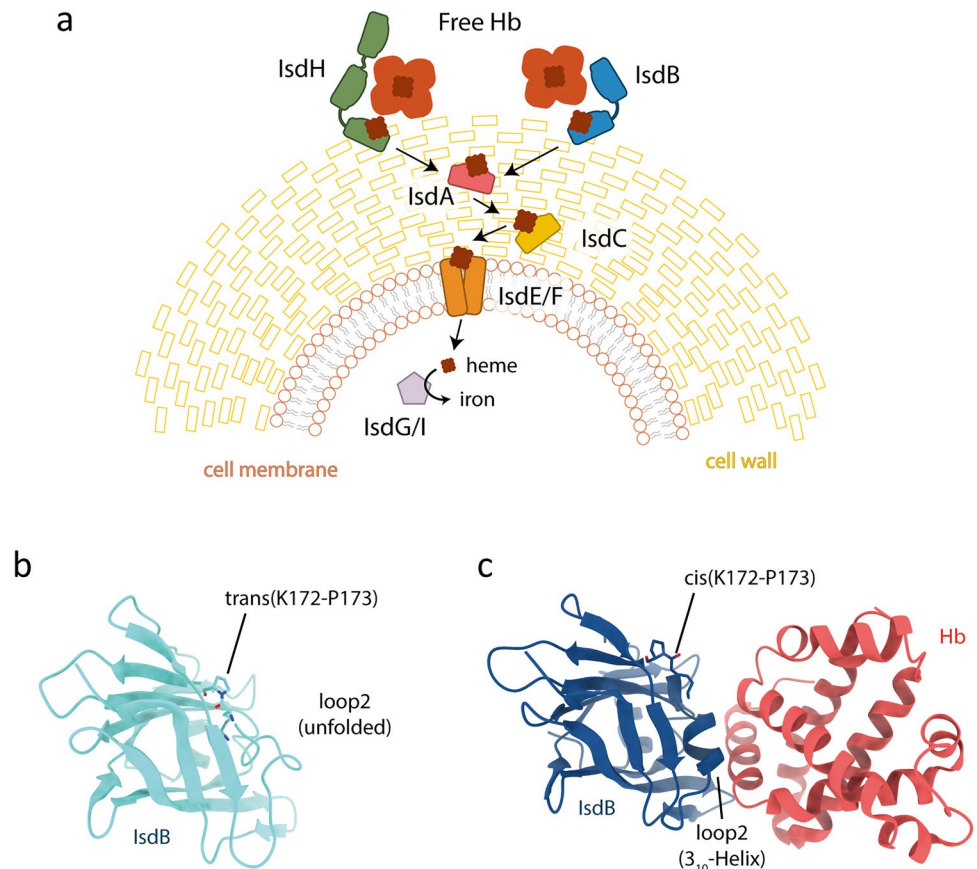
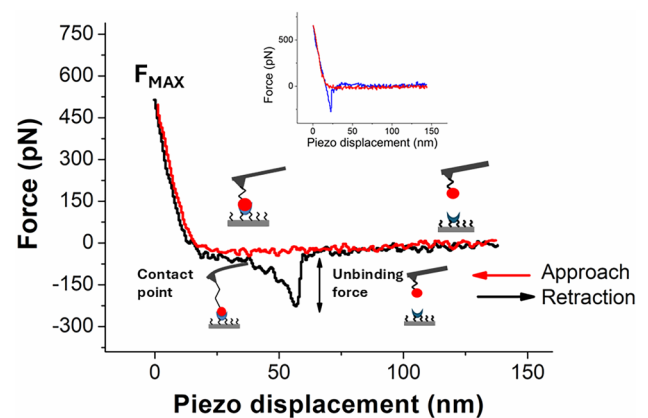


**Fig. 2** Representative force curves for a specific event and for an adhesion event (for comparison in the inset) from AFS experiment performed with a tip functionalized with IsdB<sup>P173A</sup> through a PEG linker and a substrate on which Hb molecules have been covalently anchored. The approach velocity is 50 nm/s while the retraction velocity is 350 nm/s, corresponding to a loading rate of 16.5 nN/s



formation, and host immune system evasion [4]. Among CWA proteins, the iron-regulated surface determinant (Isd) system is responsible for iron acquisition during bacterial infection and is upregulated under iron-restricted conditions [1, 5–8]. Isd comprises nine proteins (IsdA–IsdI) that act in synergy to bind the hemoglobin (Hb) released from red blood cells by bacterial hemolysins, extract heme, transport it into the cytoplasm, and release iron (Fig. 1A). IsdB is also involved in various steps of adhesion, colonization and pathogenesis in different host niches [4, 8–10]. In particular, IsdB interacts with the extracellular matrix protein vitronectin and  $\alpha\text{IIb}\beta_3$ , and  $\alpha\text{V}\beta_3$  integrins on platelets and endothelial cells [11–15]. IsdB has a modular structure formed by two NEAT iron Transporter (NEAT) domains organized in an immunoglobulin-like fold (Fig. 2B): NEAT1, involved in Hb binding, and NEAT2, which performs heme extraction [16, 17]. Of notice, heme extraction takes place selectively from the oxidized form of Hb (methemoglobin, metHb), while reduced, liganded forms of the protein (oxygenated Hb, oxyHb, and Hb bound to CO, HbCO) are resistant to heme extraction.

The three-dimensional structures of LsdB in complex with either HbCO or metHb have been recently solved by our group [18], while no three-dimensional structure of LsdB in complex with either vitronectin or integrins has ever been reported to date.

The interaction between LsdB and Hb has been also studied by atomic force spectroscopy (AFS), a nanotechnological technique that allows to investigate, under near-physiological conditions, the force regulating the interaction and the unbinding kinetics between biomolecular partners at the single-molecule level, allowing to bring out aspects hidden in bulk [19]. It was found that the unbinding process between LsdB and metHb exhibits a marked deviation from the trend observed in the largest part of biomolecular complexes when subjected to an external force. More specifically, the force required for the unbinding of the complex increases as far as higher physical stress is applied [20]. Such a behavior has been interpreted in terms of the so-called “catch bond” which is a counterintuitive phenomenon characterized by an increase of the receptor–ligand bond lifetime when a stronger external force is applied to the system. Indeed, catch bonds are opposite to slip bonds for which the application of forces to a biomolecular complex yields a destabilization, or weakening, of the intermolecular binding [20]. Catch bonds have been found in a variety of bacterial and cellular adhesion molecules [21, 22], including in the interaction of LsdB with vitronectin, integrins, and other adhesion proteins [11–15]. In SA, such an effect has been put into relationship to the control of the bacterium adhesive function during colonization and infection [23]. The occurrence of a catch bond-like trend detected in the LsdB:metHb complex has been interpreted in terms of an LsdB ability to engage in stress-dependent bonding with Hb, with this likely facilitating other biological functions besides cell adhesion. More specifically, since heme extraction from metHb is a relatively slow process, occurring on a time scale of seconds, LsdB might take advantage of complex stabilization in the shear stress conditions experienced in blood vessels. Despite the observation of catch bonds in many relevant instances, the understanding of the molecular basis of this behavior is still lagging behind. In the case of LsdB:Hb interaction, our group has previously observed that Pro173, located in the proximity of a loop in the NEAT 1 domain of LsdB that undergoes folding-upon binding to Hb, influences the affinity between the two proteins. It has to be noted that Pro173 is not directly involved in Hb binding, nor in heme extraction, which is carried out by NEAT2. Interestingly, in the structure of LsdB alone the Lys172-Pro173 bond is in *trans* configuration while when LsdB is bound to Hb this bond is in the *cis* configuration [18].

Here, with the aim to closely address the molecular mechanisms at the basis of the peculiar enhancement observed in the LsdB:Hb interaction, we have investigated by AFS the interaction between Hb and the LsdB point mutant P173A (LsdB<sup>P173A</sup>), in which Pro173 has been substituted by Ala. In contrast to proline, alanine would make *trans-cis* isomerization less favorable. Indeed, *trans-cis* isomerization is energetically unfavourable for peptide bonds involving all amino acids except Pro, since the *trans* configuration is significantly more stable than the *cis* configuration due to steric hindrance. However, for X-Pro peptide bonds, the *trans* configuration, while being still the most populated one, becomes less stable due to increased steric clashes, resulting in a lower energy barrier for isomerization [24]. Thus, the P173A mutant is expected to serve as a model of a hemophore where isomerization is disfavored. The reduction of the unbinding forces at high loading rates detected in the LsdB<sup>P173A</sup>:metHb complex offers a new perspective into the molecular mechanisms that govern the global capability of SA to attack and infect human cells.

## 2 Experimental procedures

### 2.1 Atomic force spectroscopy (AFS)

LsdB<sup>P173A</sup> and Hb molecules were covalently linked to AFM tips and glass slides, respectively, by following the same procedures used in the previous works [25–27]. Briefly, silicon nitride AFM tips with a nominal spring constant,  $k_{\text{nom}}$ , of 0.06 N/m, (cantilever D, SNL-10; Bruker Corporation, Massachusetts, USA), were irradiated with UV for 30 min and incubated with a solution of 2% (v/v) 3-mercaptopropyl-trimethoxysilane (MPTMS) (Sigma–Aldrich Co.) in toluene (99.5%, Sigma–Aldrich Co.). The silanized tips were immersed in a 1 mM solution of N-hydroxysuccinimide–polyethyleneglycol–maleimide (NHS-PEG-MAL, 3.4 kDa, hereafter PEG) (Iris Biotech, Germany) in dimethylsulfoxide (DMSO) (99.9%, Sigma–Aldrich Co.) for 3 h. The tips were incubated overnight at 4 °C with 25  $\mu\text{L}$  of 5  $\mu\text{M}$  LsdB<sup>P173A</sup> in Buffer W (0.1 M Tris, 0.15 M NaCl, 1 mM EDTA), pH 8.0 at 25 °C, for the binding between the NHS-ester groups of the PEG and the amino groups of lysines exposed on the surface of LsdB<sup>P173A</sup>. Aldehyde-functionalized glass surfaces, 1  $\text{cm}^2$  (PolyAn GmbH, Germany), were incubated with 50  $\mu\text{L}$  of 10  $\mu\text{M}$  Hb solutions in Buffer W for 4 h at 25 °C in an air-tight container for covalent binding between silane and protein amino groups. After rinsing with buffer and Milli-Q water, unreacted groups of both tips and substrates were passivated by incubation with 1 M ethanolamine hydrochloride, pH 8.5 in Milli-Q water (GE Healthcare) for 30 min at

25 °C and then rinsed with Buffer W. Measurements were immediately conducted after the glass slides functionalization; conversely, IsdB-functionalized-tips were wet stored in buffer at 4 °C in between experiments.

AFS measurements were performed at room temperature with a Nanoscope IIIa/Multimode AFM (Veeco Instruments, New York, USA), in fluid, using Buffer W saturated with N<sub>2</sub> for methHb. Force curves were collected by approaching the IsdB<sup>P173A</sup>-functionalized tip to methHb-functionalized substrate and then retracting it. The approaching phase was stopped upon reaching a preset maximum contact force value of 0.7 nN. A ramp size of 150 nm and an encounter time of 100 ms were set up. The approach was fixed at a constant velocity of 50 nm/s, while the retraction velocity was varied from 50 to 4200 nm/s. This led to several different loading rates (LRs), defined as  $dF/dt$  and given by the product of the cantilever retraction velocity ( $v$ ) and the spring constant of the system,  $k_{\text{sys}}$ , accounting for the effect of the molecules tied to the tip;  $k_{\text{sys}}$  being calculated from the slope of the retraction curve immediately before the unbinding event, for each loading rate [28]. The unbinding force  $F$ , i.e. the exerted force able to break the interaction complex, was calculated by multiplying the cantilever deflection by its effective spring constant ( $k_{\text{eff}}$ ), experimentally evaluated by the method provided in ref.[29].

Curves characterized, during the retraction phase, by sharp peaks with starting and ending points at zero deflection line, and by a nonlinear curved shape before the jump-off, which was related to the stretching features of the PEG linker, were selected as related to specific unbinding events [30]. More specifically, the nonlinear trend should be described by the Worm-Like-Chain (WLC) model with a persistence length consistent with that of the used PEG (0.36 nm), according to the procedure reported in [31]. Such a procedure also supports the selection of curves corresponding to single molecule regime [27, 29]. For curves characterized by sequentially unbinding processes (only occasionally observed), the last unbinding process was taken into consideration [19]. For each loading rate a thousand force curves were acquired from five different regions (200 curves for each region) sampled in an area of about 5  $\mu\text{m}^2$ . Each experiment was carried out by using the same functionalized tip. Experiments were conducted in triplicates. Blocking experiments were carried out by collecting force curves at the retraction velocity of 350 nm/s with the IsdB<sup>P173A</sup>-functionalized tip, which had been previously incubated with a Hb solution at 10  $\mu\text{M}$ , against the Hb-substrate in Buffer W at 25 °C.

## 2.2 Protein expression and purification

The site directed P173A mutant was prepared by standard mutagenesis techniques [32] and the correct insertion of the substitution in the coding gene verified by sequencing. The preparation of IsdB and Hb was carried out as previously described [26]. Briefly, the sequence of IsdB optimized for expression in *Escherichia coli* and carrying a C-terminal Strep-tag<sup>®</sup> II was expressed in the BL21 strain in M9 minimal medium to minimize the incorporation of heme. After bacterial lysis, IsdB was purified by affinity chromatography on a Strep-Tactin<sup>®</sup> XT (IBA Lifesciences) resin-packed column. High-molecular weight contaminants were removed by size exclusion chromatography. The purity of the final IsdB preparation was higher than 95%, with a yield of more than 100 mg L<sup>-1</sup> of cell culture. The amount of holo-IsdB was estimated as lower than 5%. Human Hb A was purified from expired blood bags of non-smoking donors obtained from a local blood transfusion center using ion exchange chromatography on a CM-Sephadex C-50 column. The oxidation state and the concentration of Hb were determined by UV-visible absorption spectroscopy exploiting the characteristic heme peaks. MethHb was prepared by treating aliquots of oxyHb with 5 mM potassium ferricyanide (Fluka, Switzerland) for 10 min at room temperature.

## 3 Results and discussion

The investigation by AFS of the interaction between IsdB<sup>P173A</sup> and methHb has been carried out by cyclically approaching and retracting the cantilever ending with a nanometric tip functionalized with IsdB<sup>P173A</sup> towards the substrate on which Hb molecules were anchored (see Fig. 2). The approach velocity has been fixed, while the retraction velocity has been varied to provide loading rates (LRs) in the 2–200 nN/m range. For each of the five different LR, a thousand curves have been collected and analyzed by sampling different regions of the substrate.

As it is well-known, the approach curves are characterized by zero deflection up to the contact point, after which intermolecular repulsive forces yield a deflection of the cantilever; an example being shown in Fig. 2 (see the red line). During this phase, the molecular partners might come into contact, with this eventually resulting in the formation of a complex. In our system, the attachment points on both the tip and the substrate are provided by the lysine residues exposed to the surface of the biomolecules; with this giving rise to some heterogeneity in the orientation of the biomolecules with a slight reduction in the probability to form a specific complex.

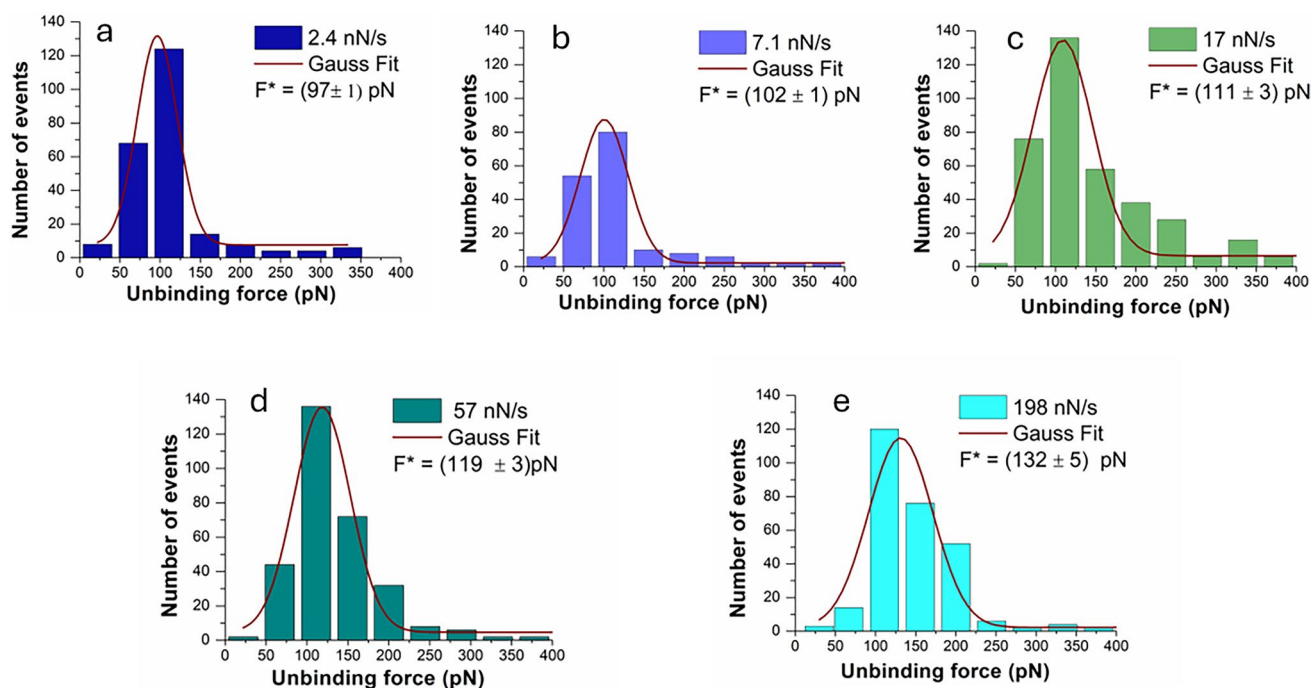
The approach phase is stopped when the cantilever applies upon the substrate a maximum contact force,  $F_{MAX}$ , whose value is established to avoid protein damage. Before retraction, the tip and the substrate are left into contact for an encounter time (here set at 100 ms), to promote the complex formation. We remark that during this time no extraction of the heme moiety from Hb is occurring [26]. The retraction curves follow the same trend of the approach one up to the contact point, after which a variety of different trends, depending on the type of interaction between the tip and substrate, can be detected (see ref. [19]). A flat curve overlapping the approaching one indicates no event (not shown). A downward deflection with a linear trend reflects nonspecific adhesion (see the blue curve in the inset of Fig. 2). Finally, a downward deflection with a nonlinear trend could result from specific events; an example being shown in Fig. 2 (see the black line). Curves whose nonlinear course is characterized by the peculiar features of PEG stretching have been attributed to specific events and selected for further analysis (for more details see the Experimental procedures). These curves show that when the applied force overcomes the intermolecular force, the complex undergoes to an unbinding process and the jump-off event allows to evaluate the corresponding unbinding force (see Fig. 2).

Figure 3 shows the histograms of the unbinding forces for curves of the  $IsdB^{P173A}$ :metHb complex, attributed to specific events, at the five LR. In all the cases, the histograms can be satisfactorily described by a single mode distribution. For each loading rate, the corresponding most probable unbinding force,  $F^*$ , has been determined by a fit to a Gaussian curve (see red continuous lines in Fig. 3). We note that the peak of the Gaussian curve is shifted towards higher values as far as higher loading rates are applied, as usually observed in the unbinding of biomolecular complexes, including the  $IsdB$ :Hb complex [19, 26].

To further assess the specificity of the observed unbinding events, we have carried out a blocking experiment in which force curves have been collected using an  $IsdB^{P173A}$ -functionalized tip, previously incubated with metHb, against metHb functionalized substrate; these experiments have been performed at the loading rate of 17 nN/s.

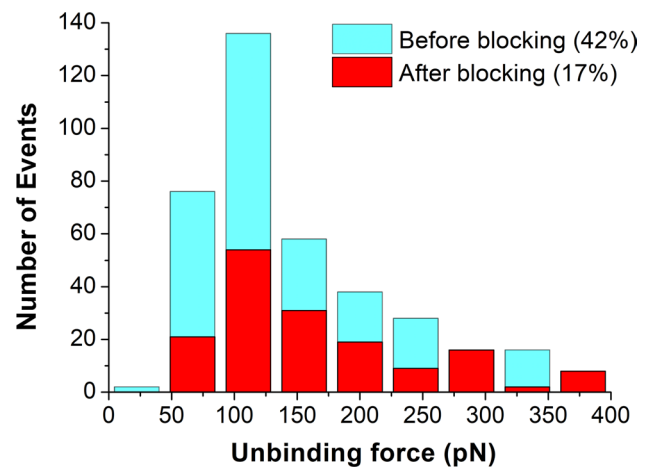
We have found that the ratio of the total number of events, attributed to specific unbinding events, over the total recorded events passes from about 42% before blocking to 17%, after blocking (Fig. 4), with a reduction of events of about 60%.

While this decrease does not definitively demonstrate specificity of the  $IsdB^{P173A}$ :metHb complex formation, it does provide support to it, in agreement with literature (see e.g. [33–35]). Furthermore, the fact that the force histograms before and after blocking (Fig. 4) show a good overlap, indicates the same nature of the corresponding interaction [36].



**Fig. 3** Histograms of the unbinding forces for the  $IsdB^{P173A}$ :metHb complex from AFS measurements carried out at five different loading rates: **a** 2.4 nN/s, **b** 7.1 nN/s, **c** 17 nN/s, **d** 57 nN/s, and **e** 198 nN/s. The most probable unbinding force value ( $F^*$ ) has been determined from the maximum of the main peak of each histogram by fitting with a Gaussian function (red lines)

**Fig. 4** Histograms of the unbinding forces for the  $\text{IsdB}^{\text{P173A}}:\text{metHb}$  complex before (cyan columns) and after (red columns) blocking, from AFS measurements carried out at a loading rate of 17 nN/s. The ratios (in percentage) of the number of events corresponding to specific unbinding processes over the total recorded events are reported



The most probable unbinding force,  $F^*$ , as extracted from the histograms in Fig. 3, is plotted as a function of the natural logarithm of loading rate, in Fig. 5. We note a linear trend throughout the loading rate range. Such a trend agrees with the prediction of the Bell-Evans model, for which the application of an external force to a complex yields a lowering of the energy barrier to be overcome for the unbinding, as a consequence of the weakening of the intermolecular binding (slip bonds). In this framework,  $F^*$  can be described by the Bell-Evans expression given by [37]:  $F^* = \frac{k_B T}{x_\beta} \ln \left[ \frac{r x_\beta}{k_{\text{off}} k_B T} \right]$ , where  $k_B$  is the Boltzmann constant,  $T$  is the absolute temperature,  $k_{\text{off}}$  is the dissociation rate constant, and  $x_\beta$  is the width of the energy barrier along the direction of the applied force. The fit by Bell-Evans equation can well describe our data, providing reliable parameters (Table 1). The  $k_{\text{off}}$  value corresponds to a characteristic lifetime,  $\tau = 1/k_{\text{off}} = 400$  s, falling in the range between adhesion and antigen/antibody complexes [38]. The  $x_\beta$  parameter, which depends on the conformation of the molecular partners, is also within the range reported for biomolecular complexes (see e.g. Tables 6.1–6.3 in ref. [39]).

These results should be discussed in connection with those recently obtained for the interaction between metHb and wild-type IsdB (Table 1).

We remark that, for the  $\text{IsdB}:\text{metHb}$  complex, the unbinding forces as a function of the natural logarithm of LR have been found to follow a linear trend up to a loading rate of 30 nN/s, while they surprisingly exhibit a marked deviation from the linear trend at higher LR values, with an enhancement of the unbinding forces (see the inset of Fig. 5). At variance, the

**Fig. 5** Bell-Evans plot given by  $F^*$  vs. the logarithm of the loading rate for the  $\text{IsdB}^{\text{P173A}}:\text{metHb}$  complex. The red continuous line is the best fit of the linear portion of the data by the model given in Bell-Evans equation [37]; the parameters extracted from the fit are reported. Inset: Bell-Evans plot for the  $\text{IsdB}:\text{metHb}$  complex with data from ref. [25]; red continuous line being a guide for eye

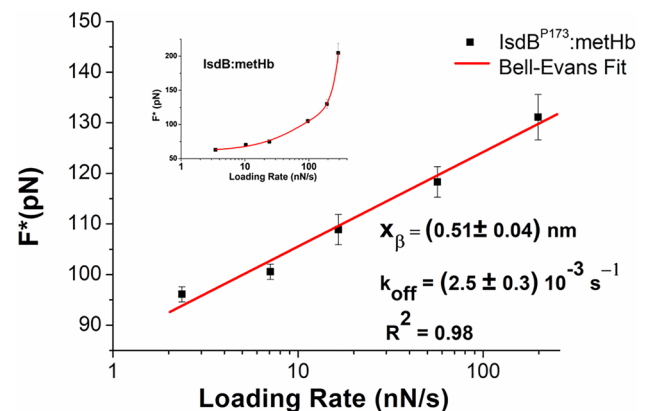


**Table 1** Comparison of data extrapolated through AFS analysis of the complex between various forms of Hb and either the wild-type IsdB or the P173A variant. (Data marked with \* are derived from the analysis of LR up to 30 nN/s)

	$k_{\text{off}}$ ( $\text{s}^{-1}$ )	$x_\beta$ (nm)
$\text{IsdB}^{\text{P173A}}:\text{metHb}$	$(2.5 \pm 0.3) \cdot 10^{-3}$	$(0.51 \pm 0.04)$
$\text{IsdB}:\text{metHb}$	$(22 \pm 4) \cdot 10^{-3}$ *	$(0.7 \pm 0.2)$ *
$\text{IsdB}:\text{HbCO}$	$(4 \pm 5) \cdot 10^{-3}$	$(0.56 \pm 0.07)$

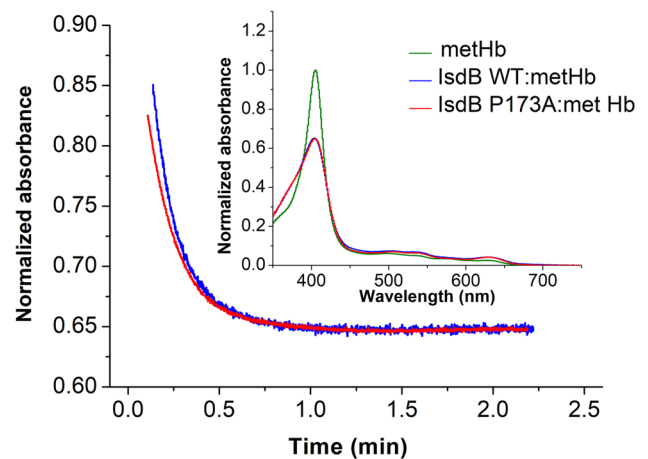
same enhancement at higher LR values is not present in the  $\text{LsdB}^{\text{P173A}}:\text{metHb}$  interaction. A comparison of the extracted parameters for the  $\text{LsdB}^{\text{P173A}}:\text{metHb}$  with those from the linear portion for the  $\text{LsdB}:\text{metHb}$  (Table 1) indicates that the values of energy barrier width are consistent in the two systems, while the  $\text{LsdB}^{\text{P173A}}$  variant is characterized by a lower  $k_{\text{off}}$  and then a longer lifetime. Globally, at low loading rates, the two complexes show a rather similar behavior in response to force application. Of notice, the analysis of data collected on  $\text{LsdB}^{\text{P173A}}:\text{metHb}$  complex shows excellent agreement with observations for the interaction of wild-type  $\text{LsdB}$  with  $\text{HbCO}$  (a form that resists heme extraction) both in terms of the dependence of  $F^*$  on LR and the extrapolated parameters by the Bell-Evans fit (Table 1). Overall, this evidence suggests that the P173A mutation did not cause gross modification of domain folding as such an event would have led to much larger deviations.

In the case of  $\text{LsdB}:\text{metHb}$  complex, the inclusion of the analysis of P173A would interestingly confirm the suggested existence of a catch bond [26]; which can be discussed in connection with the similar behavior reported for the interaction between  $\text{LsdB}$  and some adhesion proteins (e.g. vitronectin and integrins) [11, 12]. In these complexes, the force enhancement has been assumed to have evolutionarily developed to improve the colonization efficiency of host tissues even in the presence of shear forces [11]. Accordingly, the occurrence of catch bond-like behavior in the  $\text{LsdB}:\text{metHb}$  complex is expected to have a direct implication in the biological function of the hemophore. Indeed, a strengthening of the adhesion of SA under shear stress conditions could provide a further evolutionary advantage by stabilizing the complex with heme extraction-competent Hb (i.e.  $\text{metHb}$ ). On the contrary, the catch-bond behavior of  $\text{LsdB}$  is lost when it interacts with  $\text{HbCO}$ , a form of Hb resistant to extraction, implying the hemophore's ability to discern between different forms of Hb and to engage in effective interactions only when it can proceed with extraction of the cofactor. In this context, the results reported in this work point out that the absence of Pro173, which is known to isomerize following  $\text{LsdB}$  binding to Hb [18], has rendered the hemophore inefficient in recognizing the form of Hb from which it can extract heme, and thus incapable of engaging in its characteristic catch bond-like behavior. Under a structural point of view, proline isomerization has been identified as a mechanism that toggles protein conformational changes in response to mechanical stress, with the *cis* bond conversion resulting in a more stable conformation [40]. Analysis of the NEAT domains of hemophores from different bacteria indicates that proline at position 173 in  $\text{LsdB}$  is conserved in the majority of hemophores from other organisms [41, 42]. These NEAT domains can generally be classified into two types: heme-binding domains (HEBD), which feature a heme-binding motif (S/YXXXY), and Hb-binding domains (HBB), which possess a Hb-binding motif ((F/Y)YH(Y/F)). Notably, Macdonald and colleagues have clarified that HEBDs do not interact with Hb [43].

In HEBDs, the proline at the position corresponding to Pro173 in  $\text{LsdB}$  is consistently found in the *cis* configuration, regardless of whether their ligand, heme, is bound (an example can be drawn from the comparison of the NEAT2 domain of  $\text{LsdB}$  found in PDB entries 7PCH and 3RTL). To date, HBBs have only been identified in *S. aureus* (NEAT1 and NEAT2 of  $\text{LsdH}$  and NEAT1 of  $\text{LsdB}$ ) and *S. lugdunensis* (NEAT1 of  $\text{LsdB}$ ). In the case of HBBs, the presence of free NEAT domains in solution is always associated with a *trans* configuration of X-Pro bond (PDB ID 2MOQ and 2H3K), while the 3D structures where hemophores are bound to Hb show the X-Pro in *cis* configuration (PDB ID 7PCH, 5SX0, and 6TB2). In both configurations, proline interacts with surrounding residues solely through the backbone, and for this reason, the mutation to alanine is not expected to cause structural changes. The HBB sequences surrounding the investigated proline mainly differ for the amino acid preceding the residue. In  $\text{LsdB}$ , position 172 is occupied by a Lys; an Asp and a Glu are present in  $\text{LsdH}$  NEAT1 and NEAT2 domains, respectively. In the NEAT-1 domain of  $\text{LsdB}$  from *S. lugdunensis*, a Ser residue is present. The lack of structural data for  $\text{LsdB}$  from *S. lugdunensis* prevents further analysis; however, serine has a much shorter side chain compared to the amino acids found in other domains, making it likely that long-range interactions with other regions of the NEAT domain are reduced. Conversely, the Asp and Glu residues on  $\text{LsdH}$  NEAT domain have a longer side chain and might mediate long-range interactions. Interestingly, only Lys172 directly contacts the backbone of amino acids forming loop2, the major determinant for interaction with Hb, while Asp and Glu only interact with the core of the corresponding NEAT domain. This evidence allows us to speculate on the possible molecular mechanism behind the catch-bond-like behavior. In fact, it is possible that the isomerization of Pro173 following Hb binding could enable the rotation of Lys172, which in turn interacts with the backbone of loop 2, stabilizing a structure competent for Hb binding. Therefore, in the P173A mutant the same stabilization is unlikely, and it might not exhibit catch-bond-like behavior because the potential isomerization of alanine cannot provide the same stabilization as *cis* proline. Furthermore, based on these considerations,  $\text{LsdH}$  should not be expected to exhibit catch-bond like behavior, as the side chains of Asp and Glu would not form a bridge to stabilize loop 2.

Although this work only formulates a preliminary hypothesis, it lays the groundwork for understanding the structure–activity relationship behind the fascinating mechanism of catch bond-like behavior observed in the interaction between Hb and its bacterial receptor. Additionally, it can be noted that previous works on the involvement of

**Fig. 6** Spectroscopic analysis of heme extraction from metHb by WT IsdB and its P173A variant: time-dependent absorbance changes at 406 nm when IsdB is mixed with metHb. Inset: Absorption spectra of metHb before (green) and after (blue and red) the addition of tenfold molar excess of IsdB



IsdB in the interaction with human host proteins vitronectin and integrins [11, 12] did not consistently attribute the observed catch bond-like mechanism to either one of the two interacting partners. Here we demonstrate that the behavior observed for the IsdB/Hb couple is mainly due to IsdB molecular properties and is completely abrogated by a single point substitution on IsdB.

We previously observed that the P173A variant of IsdB could complete heme extraction [18], despite a decreased affinity for Hb. To further investigate the effect of the substitution on the efficiency of heme extraction, we monitored the kinetics of the process exploiting the characteristic spectroscopic signal of the cofactor. Indeed, it is well known that the transfer of heme from metHb to IsdB results in a change in the absorption spectrum of the cofactor [44]. Absorption spectra were collected before and after mixing metHb with either WT IsdB or the P173A variant, and the signal change at 406 nm was monitored (Fig. 6). The Pro > Ala substitution does not significantly affect heme acquisition by IsdB, suggesting that in a non-physiological environment, i.e. high protein concentrations and no shear stress, Pro173 does not play a critical role in the mechanism of heme extraction.

In a previous work we suggested that the Pro173 *cis-trans* isomerization could be essential for IsdB/Hb complex formation and dissociation after heme extraction [18]. Further studies will be required to assess the exact mechanism by which this event triggers selective strengthening of the IsdB:metHb complex under shear stress, while unaffected the IsdB:HbCO complex. Indeed, since the NEAT2 domain of IsdB binds Hb in front of the heme pocket and is responsible for heme extraction, it is tempting to speculate that the isomerization of Pro173 in NEAT1 is transmitted through the linker region to the NEAT2 domain, that is able to translate this conformational change in complex stabilization under shear stress, but only in the presence of metHb.

**Acknowledgements** This project was funded by “PRIN-2020—Defeat antimicrobial resistance through iron starvation in *Staphylococcus aureus* (ERASE)” (Grant 2020AE3LTA) to Stefano Bettati and Anna Rita Bizzarri.

**Author contributions** Conceptualization: Omar De Bei; Marialaura Marchetti, Barbara Campanini, Salvatore Cannistraro, Stefano Bettati, and Anna Rita Bizzarri; Methodology: Francesca Pancrazi, Francesco Lavecchia di Tocco; Formal analysis and investigation: Omar De Bei; Francesca Pancrazi, Francesco Lavecchia di Tocco; Writing—original draft preparation: Omar De Bei, Francesco Lavecchia di Tocco, Marialaura Marchetti, Barbara Campanini; Writing—review and editing: Salvatore Cannistraro, Stefano Bettati, and Anna Rita Bizzarri; Funding acquisition: Stefano Bettati, and Anna Rita Bizzarri; Resources: Stefano Bettati, and Anna Rita Bizzarri; Supervision: Barbara Campanini, Salvatore Cannistraro, Stefano Bettati, and Anna Rita Bizzarri. All the authors read and approved the manuscript.

**Funding** This project was funded by “PRIN-2020—Defeat antimicrobial resistance through iron starvation in *Staphylococcus aureus* (ERASE)” (Grant 2020AE3LTA) to Stefano Bettati and Anna Rita Bizzarri.

**Data availability** The datasets generated during and/or analyzed during the current study are available from the corresponding author on reasonable request.

**Code availability** Not applicable.

## Declarations

**Competing interests** The authors declare no competing interests.



**Open Access** This article is licensed under a Creative Commons Attribution-NonCommercial-NoDerivatives 4.0 International License, which permits any non-commercial use, sharing, distribution and reproduction in any medium or format, as long as you give appropriate credit to the original author(s) and the source, provide a link to the Creative Commons licence, and indicate if you modified the licensed material. You do not have permission under this licence to share adapted material derived from this article or parts of it. The images or other third party material in this article are included in the article's Creative Commons licence, unless indicated otherwise in a credit line to the material. If material is not included in the article's Creative Commons licence and your intended use is not permitted by statutory regulation or exceeds the permitted use, you will need to obtain permission directly from the copyright holder. To view a copy of this licence, visit <http://creativecommons.org/licenses/by-nc-nd/4.0/>.

## References

1. Marchetti M, De Bei O, Bettati S, Campanini B, Kovachka S, Gianquinto E, Spyarakis F, Ronda L. Iron metabolism at the interface between host and pathogen: from nutritional immunity to antibacterial development. *Int J Mol Sci*. 2020. <https://doi.org/10.3390/ijms21062145>.
2. Jesudason T. WHO publishes updated list of bacterial priority pathogens. *The Lancet Microbe*. 2024;5(9):100940. <https://doi.org/10.1016/j.lanmic.2024.07.003>.
3. Thomer L, Schneewind O, Missiakas D. Pathogenesis of *Staphylococcus aureus* bloodstream infections. *Annu Rev Pathol*. 2016;11:343–64. <https://doi.org/10.1146/annurev-pathol-012615-044351>.
4. Foster TJ, Geoghegan JA, Ganesh VK, Höök M. Adhesion, invasion and evasion: the many functions of the surface proteins of *Staphylococcus aureus*. *Nat Rev Microbiol*. 2014;12(1):49–62. <https://doi.org/10.1038/nrmicro3161>.
5. Bowden CFM, Chan ACK, Li EJW, Arrieta AL, Eltis LD, Murphy MEP. Structure-function analyses reveal key features in *Staphylococcus aureus* IsdB-associated unfolding of the heme-binding pocket of human hemoglobin. *J Biol Chem*. 2018;293(1):177–90. <https://doi.org/10.1074/jbc.M117.806562>.
6. Brown SA, Palmer KL, Whiteley M. Revisiting the host as a growth medium. *Nat Rev Microbiol*. 2008;6(9):657–66. <https://doi.org/10.1038/nrmicro1955>.
7. Dryla A, Hoffmann B, Gelbmann D, Giefing C, Hanner M, Meinke A, Anderson AS, Koppensteiner W, Konrat R, von Gabain A, Nagy E. High-affinity binding of the staphylococcal HarA protein to haptoglobin and hemoglobin involves a domain with an antiparallel eight-stranded beta-barrel fold. *J Bacteriol*. 2007;189(1):254–64. <https://doi.org/10.1128/jb.01366-06>.
8. Clarke SR, Andre G, Walsh EJ, Dufrière YF, Foster TJ, Foster SJ. Iron-regulated surface determinant protein A mediates adhesion of *Staphylococcus aureus* to human corneocyte envelope proteins. *Infect Immun*. 2009;77(6):2408–16. <https://doi.org/10.1128/iai.01304-08>.
9. Pishchany G, Dickey SE, Skaar EP. Subcellular localization of the *Staphylococcus aureus* heme iron transport components IsdA and IsdB. *Infect Immun*. 2009;77(7):2624–34. <https://doi.org/10.1128/iai.01531-08>.
10. Alfeo MJ, Pagotto A, Barbieri G, Foster TJ, Vanhoorelbeke K, De Filippis V, Speziale P, Pietrocola G. *Staphylococcus aureus* iron-regulated surface determinant B (IsdB) protein interacts with von Willebrand factor and promotes adherence to endothelial cells. *Sci Rep*. 2021;11(1):22799. <https://doi.org/10.1038/s41598-021-02065-w>.
11. Mathelié-Guinlet M, Viela F, Alfeo MJ, Pietrocola G, Speziale P, Dufrière YF. Single-molecule analysis demonstrates stress-enhanced binding between *Staphylococcus aureus* surface protein IsdB and host cell integrins. *Nano Lett*. 2020;20(12):8919–25. <https://doi.org/10.1021/acsnanolett.0c04015>.
12. Mathelié-Guinlet M, Viela F, Pietrocola G, Speziale P, Dufrière YF. Nanonewton forces between *Staphylococcus aureus* surface protein IsdB and vitronectin. *Nanoscale Adv*. 2020;2(12):5728–36. <https://doi.org/10.1039/D0NA00636J>.
13. Miajlovic H, Zapotoczna M, Geoghegan JA, Kerrigan SW, Speziale P, Foster TJ. Direct interaction of iron-regulated surface determinant IsdB of *Staphylococcus aureus* with the GPIIb/IIIa receptor on platelets. *Microbiol*. 2010;156(Pt 3):920–8. <https://doi.org/10.1099/mic.0.036673-0>.
14. Pietrocola G, Pellegrini A, Alfeo MJ, Marchese L, Foster TJ, Speziale P. The iron-regulated surface determinant B (IsdB) protein from *Staphylococcus aureus* acts as a receptor for the host protein vitronectin. *J Biol Chem*. 2020;295(29):10008–22. <https://doi.org/10.1074/jbc.RA120.013510>.
15. Zapotoczna M, Jevnikar Z, Miajlovic H, Kos J, Foster TJ. Iron-regulated surface determinant B (IsdB) promotes *Staphylococcus aureus* adherence to and internalization by non-phagocytic human cells. *Cell Microbiol*. 2013;15(6):1026–41. <https://doi.org/10.1111/cmi.12097>.
16. Hare SA. Diverse structural approaches to haem appropriation by pathogenic bacteria. *Biochim Biophys Acta—Proteins Proteom*. 2017;1865(4):422–33. <https://doi.org/10.1016/j.bbapap.2017.01.006>.
17. Pishchany G, Sheldon JR, Dickson CF, Alam MT, Read TD, Gell DA, Heinrichs DE, Skaar EP. IsdB-dependent hemoglobin binding is required for acquisition of heme by *Staphylococcus aureus*. *J Infect Dis*. 2013;209(11):1764–72. <https://doi.org/10.1093/infdis/jit817>.
18. De Bei O, Marchetti M, Ronda L, Gianquinto E, Lazzarato L, Chirgadze DY, Hardwick SW, Cooper LR, Spyarakis F, Luisi BF, Campanini B, Bettati S. Cryo-EM structures of staphylococcal IsdB bound to human hemoglobin reveal the process of heme extraction. *Proc Natl Acad Sci*. 2022;119(14):e2116708119. <https://doi.org/10.1073/pnas.2116708119>.
19. Bizzarri AR, Cannistraro S. The application of atomic force spectroscopy to the study of biological complexes undergoing a biorecognition process. *Chem Soc Rev*. 2010;39(2):734–49. <https://doi.org/10.1039/B811426A>.
20. Thomas WE. Mechanochemistry of receptor–ligand bonds. *Curr Opin Struct Biol*. 2009;19(1):50–5. <https://doi.org/10.1016/j.sbi.2008.12.006>.
21. Marshall BT, Long M, Piper JW, Yago T, McEver RP, Zhu C. Direct observation of catch bonds involving cell-adhesion molecules. *Nature*. 2003;423(6936):190–3. <https://doi.org/10.1038/nature01605>.
22. Thomas W. Catch bonds in adhesion. *Annu Rev Biomed Eng*. 2008;10:39–57. <https://doi.org/10.1146/annurev.bioeng.10.061807.160427>.

23. Mathelié-Guinlet M, Viela F, Alsteens D, Dufrêne YF. Stress-induced catch-bonds to enhance bacterial adhesion. *Trends Microbiol.* 2021;29(4):286–8. <https://doi.org/10.1016/j.tim.2020.11.009>.
24. Ganguly HK, Basu G. Conformational landscape of substituted prolines. *Biophys Rev.* 2020;12(1):25–39. <https://doi.org/10.1007/s12551-020-00621-8>.
25. Botti V, Cannistraro S, Bizzarri AR. Interaction of miR-155 with human serum albumin: an atomic force spectroscopy, fluorescence, FRET, and computational modelling evidence. *Int J Mol Sci.* 2022;23(18):10728. <https://doi.org/10.3390/ijms231810728>.
26. Botti V, De Bei O, Marchetti M, Campanini B, Cannistraro S, Bettati S, Bizzarri AR. Nanoscale dynamical investigation of the hemoglobin complex with the bacterial protein IsdB: is their interaction stabilized by catch bonds? *Nanoscale.* 2024;16(8):4308–16. <https://doi.org/10.1039/D3NR05241A>.
27. Moscetti I, Cannistraro S, Bizzarri AR. Probing direct interaction of oncomiR-21-3p with the tumor suppressor p53 by fluorescence, FRET and atomic force spectroscopy. *Arch Biochem Biophys.* 2019;671:35–41. <https://doi.org/10.1016/j.abb.2019.05.026>.
28. Friedsam C, Wehle AK, Kühner F, Gaub HE. Dynamic single-molecule force spectroscopy: bond rupture analysis with variable spacer length. *J Phys Condens Matter.* 2003;15(18):S1709. <https://doi.org/10.1088/0953-8984/15/18/305>.
29. Hutter JL, Bechhoefer J. Calibration of atomic-force microscope tips. *Rev Sci Instrum.* 1993;64(7):1868–73. <https://doi.org/10.1063/1.1143970>.
30. Kienberger F, Ebner A, Gruber HJ, Hinterdorfer P. Molecular recognition imaging and force spectroscopy of single biomolecules. *Acc Chem Res.* 2006;39(1):29–36. <https://doi.org/10.1021/ar050084m>.
31. Bizzarri AR, Cannistraro S. Free energy evaluation of the p53-Mdm2 complex from unbinding work measured by dynamic force spectroscopy. *Phys Chem Chem Phys.* 2011;13(7):2738–43. <https://doi.org/10.1039/C0CP01474E>.
32. Liu H, Naismith JH. An efficient one-step site-directed deletion, insertion, single and multiple-site plasmid mutagenesis protocol. *BMC Biotechnol.* 2008;8(1):91. <https://doi.org/10.1186/1472-6750-8-91>.
33. Hinterdorfer P, Dufrêne YF. Detection and localization of single molecular recognition events using atomic force microscopy. *Nat Methods.* 2006;3(5):347–55. <https://doi.org/10.1038/nmeth871>.
34. Willemsen OH, Snel MME, Kuipers L, Figdor CG, Greve J, De Grooth BG. A physical approach to reduce nonspecific adhesion in molecular recognition atomic force microscopy. *Biophys J.* 1999;76(2):716–24. [https://doi.org/10.1016/S0006-3495\(99\)77238-3](https://doi.org/10.1016/S0006-3495(99)77238-3).
35. De Paris R, Strunz T, Oroszlan K, Güntherodt H-J, Hegner M. Force spectroscopy and dynamics of the biotin avidin bond studied by scanning force microscopy. *Single Molecules.* 2000;1(4):285–90. [https://doi.org/10.1002/1438-5171\(200012\)1:4%3c285::AID-SIMO285%3e3.0.CO;2-3](https://doi.org/10.1002/1438-5171(200012)1:4%3c285::AID-SIMO285%3e3.0.CO;2-3).
36. Bonanni B, Kamruzzahan ASM, Bizzarri AR, Rankl C, Gruber HJ, Hinterdorfer P, Cannistraro S. Single molecule recognition between cytochrome C 551 and gold-immobilized Azurin by force spectroscopy. *Biophys J.* 2005;89(4):2783–91. <https://doi.org/10.1529/biophysj.105.064097>.
37. Bell GI. Models for the specific adhesion of cells to cells. *Science.* 1978;200(4342):618–27. <https://doi.org/10.1126/science.347575>.
38. Schreiber G, Haran G, Zhou HX. Fundamental aspects of protein–protein association kinetics. *Chem Rev.* 2009;109(3):839–60. <https://doi.org/10.1021/cr800373w>.
39. Bizzarri AR, Cannistraro S. *Dynamic Force Spectroscopy and Biomolecular Recognition*. Boca Raton: CRC Press; 2012.
40. Rognoni L, Möst T, Žoldák G, Rief M. Force-dependent isomerization kinetics of a highly conserved proline switch modulates the mechanosensing region of filamin. *Proc Natl Acad Sci.* 2014;111(15):5568–73. <https://doi.org/10.1073/pnas.1319448111>.
41. Andrade MA, Ciccarelli FD, Perez-Iratxeta C, Bork P. NEAT a domain duplicated in genes near the components of a putative Fe<sup>3+</sup> siderophore transporter from gram-positive pathogenic bacteria. *Genome Biol.* 2002;3(9):research00471. <https://doi.org/10.1186/gb-2002-3-9-research0047>.
42. Daou N, Buisson C, Gohar M, Vidic J, Bierne H, Kallassy M, Lereclus D, Nielsen-LeRoux C. IIsA, a unique surface protein of *Bacillus cereus* required for iron acquisition from heme, hemoglobin and ferritin. *PLoS Pathog.* 2009;5(11):e1000675. <https://doi.org/10.1371/journal.ppat.1000675>.
43. Macdonald R, Mahoney BJ, Ellis-Guardiola K, Maresso A, Clubb RT. NMR experiments redefine the hemoglobin binding properties of bacterial NEAr-iron Transporter domains. *Protein Sci.* 2019;28(8):1513–23. <https://doi.org/10.1002/pro.3662>.
44. Gianquinto E, Moscetti I, De Bei O, Campanini B, Marchetti M, Luque FJ, Cannistraro S, Ronda L, Bizzarri AR, Spyraakis F, Bettati S. Interaction of human hemoglobin and semi-hemoglobins with the *Staphylococcus aureus* hemophore IsdB: a kinetic and mechanistic insight. *Sci Rep.* 2019;9(1):18629. <https://doi.org/10.1038/s41598-019-54970-w>.

**Publisher's Note** Springer Nature remains neutral with regard to jurisdictional claims in published maps and institutional affiliations.